JOURNAL OF GEOPHYSICAL RESEARCH, VOL. 97, NO. D15, PAGES 16,473–16,479, OCTOBER 30, 1992

Deposition of Ozone to Tundra

D. J. Jacob, S.-M. Fan, S. C. Wofsy, P. A. Spiro, and P. S. Bakwin

Department of Earth and Planetary Sciences and Division of Applied Sciences, Harvard University, Cambridge, Massachusetts

J. A. Ritter, E. V. Browell, and G. L. Gregory

NASA Langley Research Center, Hampton, Virginia

D. R. Fitzjarrald and K. E. Moore

Atmospheric Sciences Research Center, State University of New York at Albany

Vertical turbulent fluxes of O_3 were measured by eddy correlation from a 12-m high tower erected over mixed tundra terrain (dry upland tundra, wet meadow tundra, and small lakes) in western Alaska during the Arctic Boundary Layer Expedition (ABLE 3A). The measurements were made continuously for 30 days in July-August 1988. The mean O_3 deposition flux was 1.3×10^{11} molecules cm^{-2} s^{-1}. The mean O_3 deposition velocity was 0.24 cm s^{-1} in the daytime and 0.12 cm s^{-1} at night. The day-to-night difference in deposition velocity was driven by both atmospheric stability and surface reactivity. The mean surface resistance to O_3 deposition was 2.6 s cm^{-1} in the daytime and 3.4 s cm^{-1} at night. The relatively low surface resistance at night is attributed to light-insensitive uptake of O_3 at dry upland tundra surfaces (mosses, lichens). The small day-to-night difference in surface resistance is attributed to additional stomatal uptake by wet meadow tundra plants in the daytime. Flux measurements from the ABLE 3A aircraft flying over the tower are in agreement with the tower data. The mean O_3 deposition flux to the world north of 60°N in July-August is estimated at 8.2×10^{10} molecules cm^{-2} s^{-1}, comparable in magnitude to the O_3 photochemical loss rate in the region derived from the ABLE 3A aircraft data. Suppression of photochemical loss by small anthropogenic inputs of nitrogen oxides could have a major effect on O_3 concentrations in the summertime Arctic troposphere.

1. Introduction

Concentrations of O_3 in the Arctic troposphere have increased by ~ 1% yr^{-1} over the past two decades, with the largest increases observed in summer [*Logan*, 1985; *Oltmans and Komhyr*, 1986]. Anthropogenic influence would be a logical explanation for these increases. However, aircraft measurements during the Arctic Boundary Layer Expedition (ABLE 3A) in July-August 1988 showed that O_3 in the region was dominantly of stratospheric rather than of pollution origin [*Browell et al.*, this issue; *Gregory et al.*, this issue]. Concentrations of nitrogen oxides (NO_x) in ABLE 3A were 10-50 ppt [*Sandholm et al.*, this issue], sufficiently low that photochemistry should provide a net sink for O_3 [*Jacob et al.*, this issue]. The budget of O_3 in the summertime Arctic troposphere appears to be regulated mainly by input from the stratosphere, and losses from photochemistry and deposition.

One possible mechanism for anthropogenic perturbation to O_3 levels in the Arctic troposphere is by partial suppression of the photochemical sink due to small enhancements of NO_x. The presence of NO_x at the low levels observed in ABLE 3A may have slowed down the photochemical loss rate of O_3 by a factor of 2.5 relative to a NO_x-free atmosphere [*Jacob et al.*, this issue]. A substantial fraction of the NO_x appeared to be anthropogenic [*Singh et al.*, this issue]. The sensitivity of the regional O_3 budget to changes in the photochemical loss rate depends however critically on the rate of loss by deposition. If deposition dominates over photochemistry as a sink for O_3 in the Arctic, then suppression of the photochemical sink is of little consequence.

We report here eddy correlation measurements of O_3 deposition fluxes to tundra during the ABLE 3A expedition. Tundra occupies 42% of total land north of 60°N [*Matthews*, 1983]; the efficiency of O_3 uptake at tundra surfaces is therefore an important element in constructing a tropospheric O_3 budget for the Arctic. Experimental methods are described in section 2. Surface resistances for O_3 deposition to tundra are derived in section 3. Flux measurements from tower and aircraft are compared in section 4. The O_3 deposition flux to the Arctic in summer is estimated in section 5, and is compared to the photochemical loss rate of O_3 computed from the ABLE 3A aircraft data. Conclusions are in section 6.

2. Experimental Methods

The measurements were made from the top of a 12-m high tower erected 40 km north of Bethel, Alaska, in the Yukon Delta National Wildlife Refuge (61°05.41' N, 162°00.92' W). The measurements were made continuously for 30 days from July 14 to August 12, 1988. Flat tundra terrain extended for several tens of kilometers in all directions around the tower and consisted of a fine mosaic of dry upland tundra (lichen-moss), wet meadow tundra (watersedge), and small lakes. The height of the tundra canopy was 5-15 cm, with shrubs up to 1 m in height in some of the wetter areas. The footprint (or fetch) sampled by the tower at 12-m altitude extended from 50 to 1000 m upwind according to Gaussian plume calculations [*Fan et al.*, this issue]. The distribution of surface types in the tower footprint was inhomogeneous, as shown in Figure 1. Two lakes occupied about half of the footprint in the NE sector, while the SE sector was relatively dry. Wet meadow tundra was most abundant to the west. The most frequent wind

Paper number 91JD02696.
0148-0227/92/91JD-02696$05.00

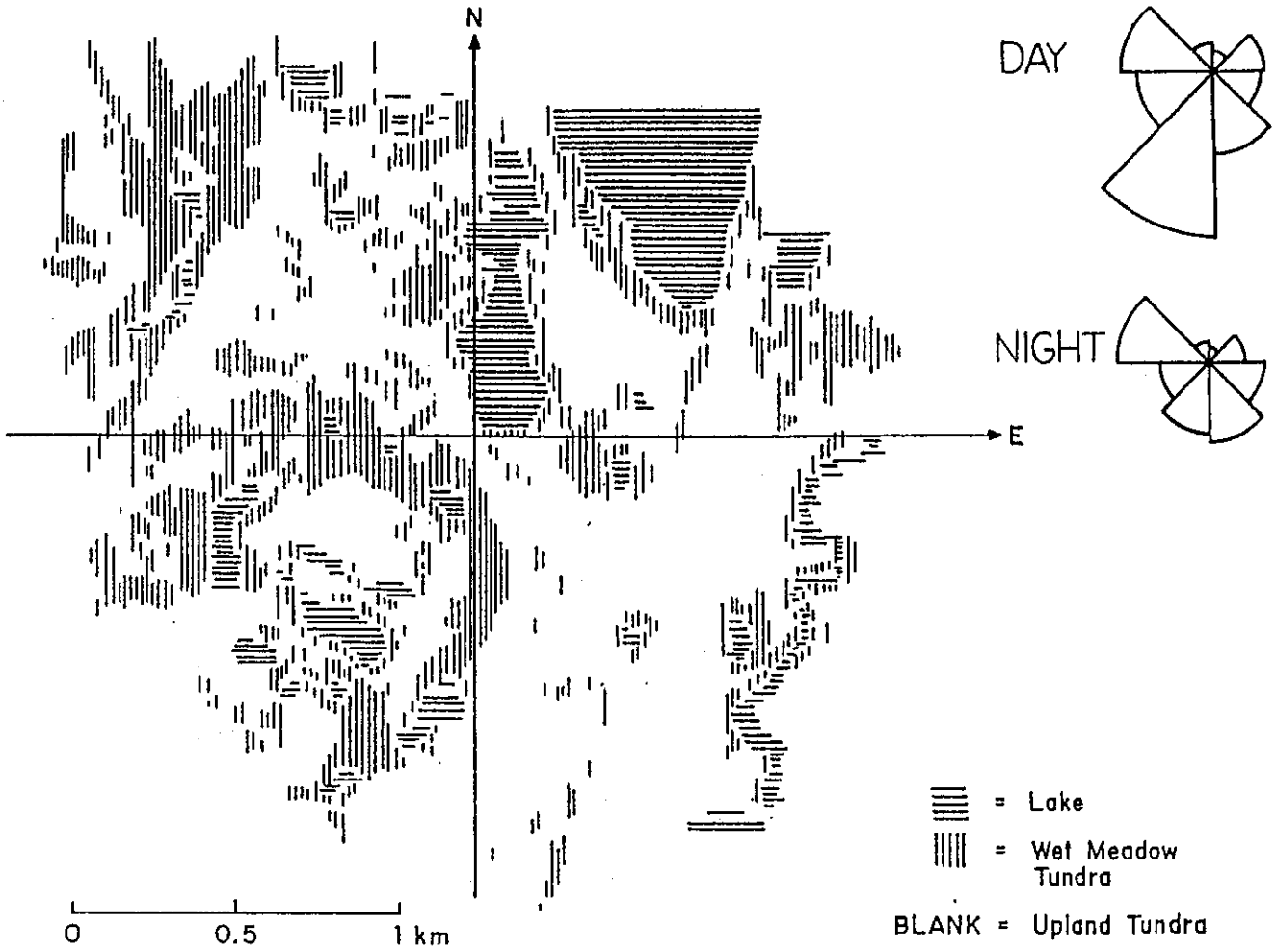

Fig. 1. Map of surface types around the ABLE 3A tower, constructed by D. Bartlett (University of New Hampshire) from satellite data with 20x20 m^2 resolution. The tower is located at the origin. Wind direction frequencies are shown for the O_3 flux measurement periods, with the radius of each 45°-wide wind sector proportional to the number of hourly mean observations in that sector.

direction was SSW in the daytime and WNW at night, but the variance was large (Figure 1).

The vertical turbulent flux of O_3, F, was computed from the covariance of fast-response measurements of vertical wind velocity (w) and O_3 concentrations (C) over an averaging time Δt = 60 min:

$$F = \frac{1}{\Delta t}\int_0^{\Delta t} w'C'dt \quad (1)$$

where the primes represent deviations from the mean. The values of w' and C' were computed relative to 4-min running means centered on the point of calculation. The 60-min averaging time allows sampling over a large number of eddies while providing reasonable resolution of the change in flux with time.

Vertical wind velocities were measured with a fast-response (10 Hz) three-axis sonic anemometer (Applied Technologies, Inc.) mounted at the end of a beam extending 1 m horizontally from the top of the tower. The O_3 sampling inlet was a Teflon tube 0.3 cm internal diameter, located on the beam 0.5 m away from the anemometer and pointing downwards. The sonic anemometer and the gas inlet were rotated using a remotely operated electric motor to keep the anemometer upwind of the tower. The coordinate frame for w' was rotated as described by *McMillen* [1988]. Concentrations of O_3 were measured using a modified C_2H_4 luminescence instrument with a 90% response time of 0.8 s [*Gregory et al.*, 1983, 1988]. The instrument gain was obtained by comparison with a Dasibi 1003-AH UV photometer. Data for w and C were acquired at 8 Hz. Time delays in the O_3 concentration measurements were determined by turning on and off an O_3 generator (Hg vapor lamp) placed near the inlet, and by analyzing the cross-correlation function between w and C [*Fan et al.*, 1990].

Contributions to the O_3 flux from frequencies > 0.6 Hz could not be resolved due to the response time of the O_3 instrument. The magnitude of the associated error was assessed using measurements of the sensible heat flux, for which the instrument bandpass exceeded 10 Hz. The heat flux data were smoothed using a filter with the same bandpass as the O_3 instrument [*Hicks and McMillen*, 1988]; on average less than 5% of the flux was lost in the daytime, and less than 10% was lost at night under neutral to moderately stable conditions [*Fan et al.*, this issue; *Fitzjarrald and Moore*, this issue]. Losses under very stable conditions could not be evaluated properly because the fluxes were small. Additional tests were made that showed negligible errors associated with selection of averaging interval or instrumental high-frequency noise [*Fan*, 1991]. Density corrections were not needed because O_3 mixing ratios (not densities) were measured. The overall uncertainty on the measurement of F is estimated to be ± 15%, and the detection limit is estimated to be 3×10^9 molecules cm^{-2} s^{-1} [*Fan*, 1991].

Wind speed, wind direction, temperature, momentum flux, and sensible heat flux were measured continuously at the top of the tower [*Fitzjarrald and Moore*, this issue]. Concentrations of O_3 and NO_x were measured continuously in sequence at eight altitude levels (11.0, 8.4, 6.0, 4.3, 3.1, 1.4, 0.5, and 0.05 m), with a 30-minute time interval between measurements at the highest and lowest levels. The O_3 and NO_x concentration data are discussed in detail by *Bakwin et al.* [this issue]. Concentrations of O_3 were typically in the range 10-30 ppb, while concentrations of NO_x were typically less than 0.02 ppb; we can therefore neglect perturbations to the O_3 flux caused by adjustment of the O_3/NO_2 photochemical equilibrium [*Lenschow*, 1982].

All times will be given as solar time (ST), defined by a maximum solar elevation at noon. Sunrise was at 0310 ST on July 14 and at 0415 ST on August 12. Solar time lagged 3 hours behind local time.

3. RESULTS

General Observations

A total of 673 hourly average fluxes were measured during the expedition. The fluxes are given as positive when pointing upwards, following usual convention; thus F is in general negative. Figure 2 shows the mean diurnal variation of F for the 30-day period from July 14 to August 12. No significant secular variation of F was observed over that period. The mean value was -1.3×10^{11} molecules cm^{-2} s^{-1}. The strongest fluxes were in the daytime.

Figure 2 also shows the mean diurnal variations of the O_3 concentration at 12-m altitude, C, and of the deposition velocity, $V_d = -F/C$. The O_3 concentrations were minimum in early morning and maximum in late afternoon, reflecting the entrainment of O_3 from aloft during daytime growth of the mixed layer [*Bakwin et al.*, this issue]. Means and standard deviations of V_d were 0.24 ± 0.10 cm s^{-1} in the daytime and 0.12 ± 0.10 cm s^{-1} at night; the day-to-night difference is significant at the 99% level of confidence.

The dependence of V_d on wind direction is shown in Figure 3. Values in the NNE sector were low, possibly due to the lakes in the tower footprint. Deposition of O_3 to water surfaces is known to be slow [*Wesely et al.*, 1981]. The highest values of V_d were in the relatively dry SE sectors. The SSW sector contained the largest number of observations; the diurnal variation of V_d for that sector (dotted line in Figure 2) is similar to that in the full data set, indicating that wind direction was not a major factor determining the diurnal variation of V_d. Atmospheric stability and surface reactivity were more important in that regard, as discussed below.

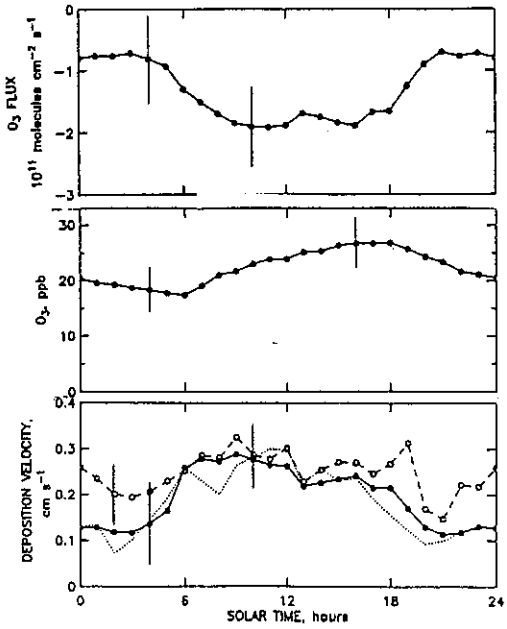

Fig. 2. Diurnal variations of the O_3 vertical turbulent flux F, the O_3 concentration C, and the O_3 deposition velocity V_d at 12-m altitude on the ABLE 3A tower. Values are means and representative standard deviations for the 30-day period from July 14 to August 12, 1988. Solar time (ST in the text) is defined by a maximum solar elevation at noon. Deposition velocities in the bottom panel are for (1) the full data set (solid line), (2) winds from the SSW sector only (dotted line), and (3) the reduced data set satisfying criteria of homogeneous and stationary turbulence (dashed line).

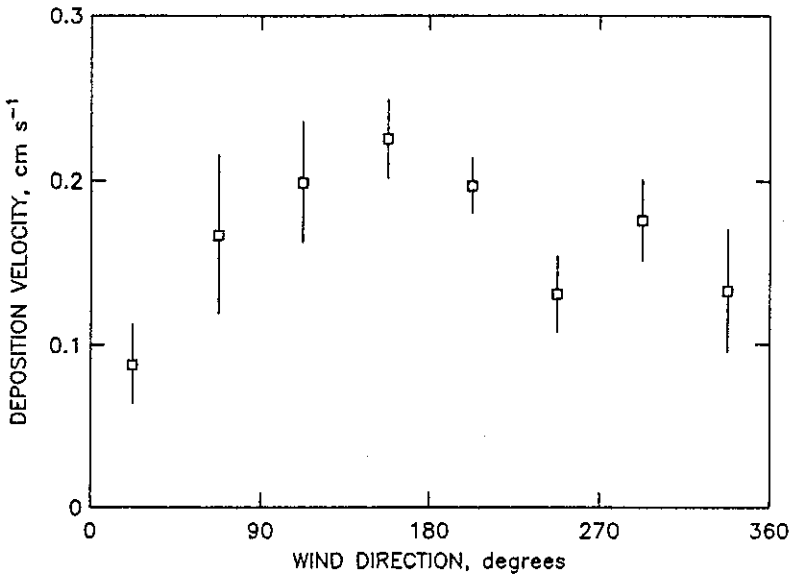

Fig. 3. Dependence of the O_3 deposition velocity on wind direction. Values are means and standard errors on the means in each 45°-wide wind sector for the full data set.

Selection of Periods of Homogeneous and Stationary Turbulence

Interpretation of V_d in terms of surface properties is facilitated if turbulence in the 0-12 m column is homogeneous and stationary. In that case, V_d is dependent only on the vertical resistance to mass transfer below 12 m (aerodynamic resistance) and on the reactivity of O_3 at the surface. The aerodynamic resistance can be computed using Monin-Obukhov (MO) similarity [*Wesely and Hicks*, 1977]. The residual surface resistance is a characteristic of the tundra terrain in the tower footprint, and can be extrapolated to other tundra surfaces.

We identify periods for which MO similarity is applicable by comparing the measured wind speed u_{OBS} at h = 12 m altitude to the value u_{MO} computed from similarity:

$$u_{MO} = \frac{u^*}{k}\int_{z_o}^{h}\frac{\phi_M(\zeta)dz}{z} \quad (2a)$$

with

$$\zeta = \frac{z-d}{L} \quad (2b)$$

and

$$\phi_M(\zeta) = (1-15\zeta)^{-1/4} \qquad \zeta < 0 \quad (2c)$$

$$\phi_M(\zeta) = 1+4.7\zeta \qquad \zeta > 0 \quad (2d)$$

Here u^* is the friction velocity, k = 0.4 is the von Karman constant, z_o is the roughness height, d is the displacement height, L is the MO length, and $\phi_M(\zeta)$ is the stability correction function for momentum [*Businger et al.*, 1971]. Values of u^* and L were computed from hourly mean tower data for momentum and sensible heat fluxes [*Fitzjarrald and Moore*, this issue]; median values of L were -10 m in the daytime and 30 m at night. The roughness height measured at the tower was 0.5 cm, independent of wind direction [*Fitzjarrald and Moore*, this issue]. The displacement height d is typically 70-80% of canopy height [*Brutsaert*, 1982], and we assume here d = 0.1 m; results are insensitive to the exact value.

Figure 4 shows the frequency distribution of the ratio u_{OBS}/u_{MO} for all hourly periods when concurrent data for F, u^*, and L were available (n = 536). High ratios are found in a number of cases, representing strongly stratified conditions. We require a 20% fit to MO similarity, i.e., a ratio in the range 0.8 to 1.2, and are left with n = 357 hourly periods for which MO similarity is considered verified.

Stationarity of the O_3 flux in the 0-12 m column is verified by comparing F to the accumulation rate Γ of O_3 in the column:

$$\Gamma = \int_0^h \frac{\partial C(z)}{\partial t}dz \quad (3)$$

where $C(z)$ is the O_3 concentration at altitude z. We compute Γ from the O_3 concentration profiles measured at the tower at 30-min intervals. Adopting as criterion $|\Gamma| < 0.2\,|F|$, we reject 40 of the 357 hourly periods that satisfy the MO similarity criterion. Another 88 hourly periods are rejected because vertical profiles of O_3 concentrations were not measured (and hence Γ could not be computed).

We are finally left with n = 229 hourly average measurements of F representing the actual surface flux of O_3 to the tower footprint under conditions when MO similarity is applicable. The diurnal variation of V_d for this reduced data set is shown as the dashed line in Figure 2. Values are higher than in the full data set, particularly at night, because the MO similarity criterion excludes periods of strong stratification. The mean day-to-night difference of V_d in the reduced data set is 0.07 cm s^{-1}, as compared to 0.12 cm s^{-1} in the full data set. We conclude that stratification of the atmosphere at night was an important factor contributing to the diurnal variation of V_d in the full data set.

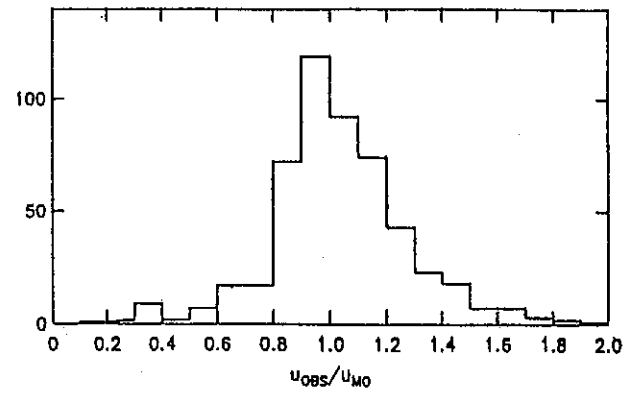

Fig. 4. Frequency distribution of the ratio u_{OBS}/u_{MO}, where u_{OBS} is the observed wind speed at 12-m altitude and u_{MO} is the wind speed computed from Monin-Obukhov similarity using equation (2). Data are from the 536 hourly periods when concurrent measurements of F, u^*, and L were available. Ratios higher than 2 were found for 21 of the periods (not shown).

Surface Resistance to Ozone Deposition

The surface resistance R_c to O_3 deposition was derived from the reduced data set satisfying MO similarity (n = 229) by subtracting aerodynamic contributions from the total resistance to deposition $R = 1/V_d$:

$$R_c = R - R_a - R_b \quad (4)$$

The aerodynamic resistance R_a between h = 12 m and z_0 was computed from MO similarity:

$$R_a = \frac{1}{ku^*}\int_{z_o}^{h}\frac{\phi_H(\zeta)dz}{z} \quad (5a)$$

where $\phi_H(\zeta)$ is the stability correction function for heat [*Businger et al.*, 1971]:

$$\phi_H(\zeta) = 0.74(1-9\zeta)^{-1/2} \qquad \zeta < 0 \quad (5b)$$

$$\phi_H(\zeta) = 0.74 + 4.7\zeta \qquad \zeta > 0 \quad (5c)$$

The boundary resistance R_b accounts for the transfer of O_3 from z_o to the deposition surfaces, and is computed following *Wesely and Hicks* [1977]:

$$R_b = \frac{2}{ku^*}\left(\frac{\kappa}{D_g}\right)^{2/3} \quad (6)$$

where κ = 0.2 cm^2 s^{-1} is the thermal diffusivity of air and D_g = 0.13 cm^2 s^{-1} is the molecular diffusivity of O_3. The cumulative contributions of R_a, R_b, and R_c to the total resistance R are shown in Figure 5 as a function of time of day. We see that deposition is limited by the surface resistance at all times. The nighttime values of R_a are relatively low because strongly stratified periods were excluded from the reduced data set.

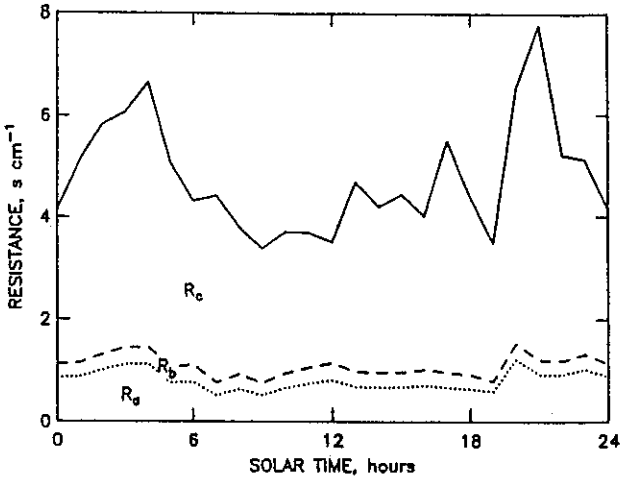

Fig. 5. Cumulative contributions of the individual resistances R_a, R_b, and R_c to the total resistance to deposition $R = 1/V_d = R_a + R_b + R_c$. Values are means for each hour of the day, for the reduced data set satisfying criteria of homogeneous and stationary turbulence.

For further data analysis we replace R_c by the surface conductance $g_c = 1/R_c$, which provides better statistics (statistics on R_c are affected by occasional high values). Figure 6 shows the dependence of g_c on wind direction, separately for day and night. Low values are found in the two northern sectors, due perhaps to the adjacent lake but corresponding to only a small number of points ($n = 9$). Values in the eastern sectors are somewhat higher than in the western sectors, possibly reflecting the drier terrain.

We view the data taken outside the two northern sectors as representative of the mixed tundra terrain in the area. Means and standard deviations of g_c for that ensemble are 0.38± 0.16 cm s^{-1} in the daytime ($n = 149$) and 0.29 ± 0.12 cm s^{-1} at night ($n = 71$). The mean day-to-night difference Δg_c is 0.09 ± 0.02 cm s^{-1}, small but significant at the 99% level of confidence.

The relatively high value of g_c at night, and the small day-to-night difference Δg_c, suggest that O_3 deposition took place mostly at dry upland tundra surfaces (either vegetation or the ground).

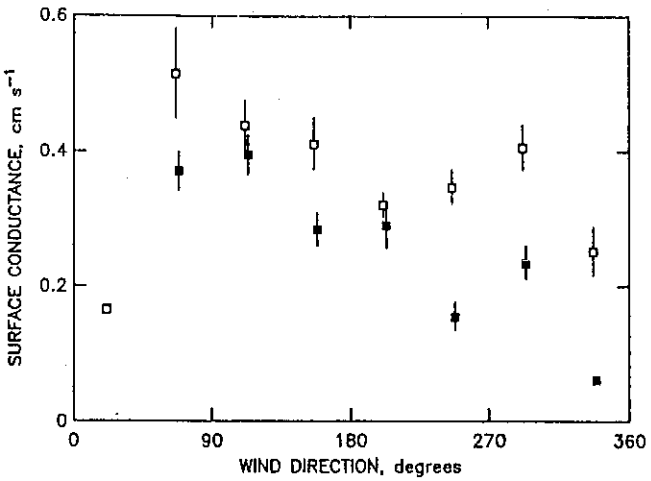

Fig. 6. Surface conductances for O_3 deposition to the ABLE 3A tower footprint, as a function of wind direction and separately for day (open squares) and night (black squares). Values are means and standard errors on the means in each 45°-wide wind sector for the reduced data set satisfying criteria of homogeneous and stationary turbulence. The 0°-45° sector in the daytime and the 315°-360° sector at night each contain only one observation. There were no observations in the 0°-45° sector at night.

Mosses and lichens, which cover most of the dry upland tundra surface, have little internal control over water vapor or CO_2 exchange [*Oechel*, 1976; *Lechowicz*, 1981, 1982; *Chapin and Shaver*, 1985]. The surface conductance for O_3 deposition to dry upland tundra may therefore vary little with time of day. In contrast, the surface conductance for O_3 deposition to wet meadow tundra should vary strongly between day and night due to stomatal closure of the wet meadow tundra plants at night. *Stoner and Miller* [1975] measured stomatal and cuticular conductances for water vapor exchange in a number of wet meadow tundra plants; they found stomatal conductances g_i in the range 0.3-1 cm s^{-1} per cm^2 of leaf depending on the plant, and very low cuticular conductances (typically 0.025 cm s^{-1} per cm^2 of leaf). The day-to-night variation of g_c resulting from the stomatal activity of wet meadow tundra plants can be estimated simply as follows:

$$\Delta g_c = f \Lambda \alpha g_i \qquad (7)$$

where $f \approx 0.3$ is the fractional area of wet meadow tundra in the tower footprint [*Fan et al.*, this issue], $\Lambda \approx 1$ is the leaf area index of wet meadow tundra [*Miller et al.*, 1976], and $\alpha = 0.6$ is the ratio of the molecular diffusivities of O_3 and H_2O needed to scale g_i [*Hicks et al.*, 1987]. Equation (7) yields values for Δg_c in the range 0.05-0.18 cm s^{-1}, consistent with observations. Some further evidence for a stomatal influence on O_3 uptake is offered by the larger values of Δg_c in the relatively wet western sectors than in the relatively dry eastern sectors (Figure 6).

4. Comparison With Aircraft Observations

Vertical turbulent fluxes of O_3 were measured from the ABLE 3A aircraft flying above the tower on July 28 and August 9 [*Ritter et al.*, this issue]. The July 28 measurements consist of a vertical profile of O_3 fluxes in the mixed layer at 0945-1040 ST, averaged horizontally over a 100 km flight track centered at the tower (Figure 7). The increase of the downward flux with altitude in Figure

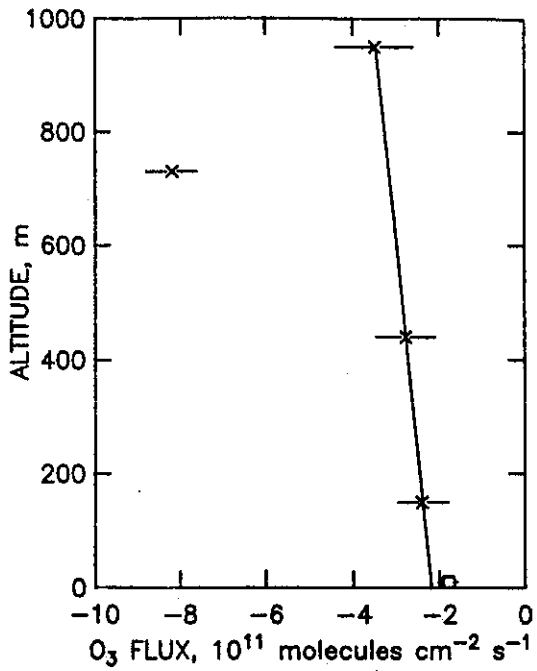

Fig. 7. Vertical turbulent fluxes of O_3 measured above the ABLE 3A tower at 0945-1040 ST on July 28. Measurements from the aircraft at four altitudes (crosses) are compared to the concurrent measurement at the tower (square). Error bars indicate measurement uncertainties. The line is a fit to the aircraft data ignoring the anomalous point at 730 m altitude.

7 reflects the entrainment of O_3 at the top of the rapidly growing mixed layer. Linear extrapolation of the aircraft data to the surface, ignoring the anomalous point at 730 m altitude, suggests a downward flux 20% higher than concurrently measured at the tower. The difference is within the uncertainty in the extrapolation.

The August 9 aircraft measurements were made at 10-15 ST during a series of flight legs at 150 m altitude criss-crossing the tundra terrain around the tower. The mean O_3 flux measured above the tower was -2.3×10^{11} molecules cm^{-2} s^{-1}, consistent with concurrent tower measurements indicating a mean flux of -2.0×10^{11} molecules cm^{-2} s^{-1}.

The agreement between the fluxes measured from tower and aircraft suggests that the surface resistances computed in the previous section are representative of the mixed tundra terrain around the tower over a scale of several tens of kilometers. We attempt in the next section to extrapolate our surface resistance data globally to all tundra surfaces.

5. OZONE DEPOSITION TO THE ARCTIC

To our knowledge, the only measurements previously reported for O_3 deposition to tundra are those of *Kelley and McTaggart-Cowan* [1968] near Barrow, Alaska, in August 1966. These authors measured vertical profiles of O_3 concentrations and wind speeds in the 0-4 m column, and derived O_3 fluxes when conditions were presumed neutral (as diagnosed from the temperature profiles). Ten flux measurements were reported which ranged from -7×10^{11} to 8×10^{11} molecules cm^{-2} s^{-1}, corresponding to deposition velocities in the range -0.4 to 0.6 cm s^{-1}. Three of the ten flux values were positive (upward), strongly suggestive of a measurement problem.

We estimate here the mean O_3 deposition flux to the world north of 60°N in July-August by extrapolating our surface resistance data to all tundra surfaces, and using literature data to estimate O_3 deposition to other surfaces. Table 1 shows the distribution of surface types north of 60°N [*Matthews*, 1983]. Tundra accounts for 18% of the total surface (42% of the land). Surface resistances to tundra are taken from section 3 as 2.6 s cm^{-1} in the daytime and 3.4 s cm^{-1} at night. Surface resistances to other vegetated land surfaces are computed following *Wesely* [1989] as the sum of stomatal, cuticular, and ground resistances placed in parallel; the formulations given by *Wesely* [1989] for these resistances depend on local temperature and solar irradiance, which are obtained from a general circulation model simulation with 4°x5° resolution and full diurnal cycle [*Hansen et al.*, 1983]. Aerodynamic resistances over all land surfaces are also computed from the general circulation model using equations (5) and (6). Fixed deposition velocities of 0.025 cm s^{-1} are assumed over oceans [*Kawa and Pearson*, 1989] and over ice [*Wesely et al.*, 1981].

The regional average deposition velocities computed for each surface type are listed in Table 1. Deposition velocities over forests and tundra are of comparable magnitude, because the more efficient stomatal uptake by forests in the daytime is balanced at night by high cuticular resistances and by the stability of the canopy which inhibits transfer to the ground. Deposition velocities over shrub, grassland, and cultivated land are relatively high but the corresponding areas are small. The average deposition velocity north of 60°N is estimated to be 0.11 cm s^{-1} (referenced to 200 m altitude). Assuming an O_3 concentration of 30 ppb at that altitude, based on data from ABLE 3A survey flights [*Gregory et al.*, this issue], we obtain an average deposition flux of 8.2×10^{10} molecules cm^{-2} s^{-1}. By comparison, *Jacob et al.* [this issue] calculated a 24-hour average O_3 photochemical loss rate of 8.0×10^{10} molecules cm^{-2} s^{-1} for the 0-6 km column during ABLE 3A. It thus appears that deposition and photochemistry provide sinks of comparable magnitude for O_3 in the summertime Arctic troposphere. The average 0-6 km O_3 column concentration in ABLE 3A was 6.4×10^{17} molecules cm^{-2} s^{-1} [*Gregory et al.*, this issue], from which we deduce an O_3 column lifetime of 46 days. This lifetime is sufficiently short that O_3 concentrations should be highly sensitive to perturbation of the photochemical sink by small anthropogenic enhancements of NO_x.

TABLE 1. Average Deposition Velocity of O_3 North of 60°N in Summer

Surface Type	Total Area,%	Deposition Velocity, cm s^{-1}
Tundra	17.5	0.20
Deciduous forest	10.6	0.26
Coniferous forest	11.2	0.23
Shrub	1.7	0.31
Grassland	0.2	0.42
Cultivated	0.1	0.43
Ocean/ice	58.7	0.025
World north of 60°N	100	0.11

The deposition velocities over each surface type are averages for July-August referenced to 200-m altitude.

6. CONCLUSIONS

Deposition fluxes of O_3 were measured at 12-m altitude over mixed tundra terrain in western Alaska during ABLE 3A. The mean deposition flux was 1.3×10^{11} molecules cm^{-2} s^{-1} for a 30-day period in July-August 1988. The mean deposition velocity was 0.24 cm s^{-1} in the daytime and 0.12 cm s^{-1} at night. The day-to-night difference in deposition velocity was driven by both atmospheric stability and surface reactivity.

A reduced data set was compiled for periods satisfying criteria of homogeneous and stationary turbulence. From this reduced data set we derived average surface resistances for O_3 deposition to tundra of 0.26 s cm^{-1} in the daytime and 0.34 s cm^{-1} at night. Most of the O_3 deposition appeared to take place at dry upland tundra surfaces, with no significant diurnal variation in surface resistance. The small day-to-night difference of surface resistance is attributed to additional stomatal uptake of O_3 by wet meadow tundra plants in the daytime.

The O_3 fluxes measured at the tower were consistent with flux measurements from the ABLE 3A aircraft flying in the mixed layer above the tower. The surface resistances to O_3 deposition computed from the tower data may therefore be viewed as representative of the terrain surrounding the tower over a scale of tens of kilometers.

An average O_3 deposition flux of 8.2×10^{10} molecules cm^{-2} s^{-1} is estimated for the world north of 60°N in summer. This value is of comparable magnitude to the 24-hour average O_3 photochemical loss rate in the 0-6 km column derived by modeling of the ABLE 3A aircraft data. The resulting atmospheric lifetime of O_3 in the 0-6 km column over the Arctic in summer is estimated at 46 days. Partial suppression of the photochemical sink by small anthropogenic inputs of NO_x could possibly explain the secular increase of O_3 concentrations observed in the Arctic troposphere over the past two decades.

Acknowledgments. This work was supported by National Science Foundation grants NSF-ATM-8858074 and NSF-ATM-8921119 to Harvard University, by a Packard Foundation Fellowship to D.J.J., by an Alexander Host Foundation Fellowship to P.S.B., and by grants from the Tropospheric Chemistry Program of the National Aeronautics and Space Ad-

ministration to participating scientists. Helpful discussions with K. Bartlett (University of New Hampshire), and field and logistical support from J. Hoell and J. Drewry (NASA-Langley), are gratefully acknowledged.

REFERENCES

Bakwin, P. S., S. C. Wofsy, S.-M. Fan, and D. R. Fitzjarrald, Measurements of NO_x and NO_y concentrations and fluxes over Arctic tundra, *J. Geophys. Res.*, this issue.

Browell, E.V., C. F. Butler, S. A. Kooi, R. C. Harriss, and G. L. Gregory, Large-scale variability of ozone and aerosols in the summertime and sub-Arctic troposphere, *J. Geophys. Res.*, this issue.

Brutsaert, W., *Evaporation into the Atmosphere*, D. Reidel, Hingham, Mass., 1982.

Businger, J. A., J. C. Wyngaard, Y. Izumi, and E. F. Bradley, Flux-profile relationships in the atmospheric surface layer, *J. Atmos. Sci., 28*, 181-189, 1971.

Chapin, F. S., III, and G. R. Shaver, Arctic, in *Physiological Ecology of North American Plant Communities*, edited by B. F. Chabot and H. A. Mooney, Chapman and Hall, New York, 1985.

Fan, S.-M., Atmosphere-biosphere exchange of CH_4, CO_2, and O_3, Ph.D. thesis, Harvard University, Cambridge, Mass., 1991.

Fan, S.-M., S. C. Wofsy, P. S. Bakwin, D. J. Jacob, and D. R. Fitzjarrald, Atmosphere-biosphere exchange of CO_2 and O_3 in the central Amazon forest, *J. Geophys. Res., 95*, 16,851-16,865, 1990.

Fan, S.-M., S. C. Wofsy, P. S. Bakwin, D. J. Jacob, S. M. Anderson, P. L. Kebabian, J. B. McManus, C. E. Kolb, and D. R. Fitzjarrald, Micrometeorological measurements of CH_4 and CO_2 exchange between the atmosphere and subarctic tundra, *J. Geophys. Res.*, this issue.

Fitzjarrald, D. R., and K. E. Moore, Turbulent transports over tundra, *J. Geophys. Res.*, this issue.

Gregory, G. L., C. H. Hudgins, and R. A. Edahl, Jr., Laboratory evaluation of an airborne ozone instrument which compensates for altitude/sensitivity effects, *Environ. Sci. Technol., 17*, 100-103, 1983.

Gregory, G. L., E. V. Browell, and L. S. Warren, Boundary layer ozone: an airborne survey above the Amazon Basin, *J. Geophys. Res., 93*, 1452-1468, 1988.

Gregory, G. L., B. Anderson, L. B. Warren, E. V. Browell, D. Bagwell, and C. H. Hudgins, Tropospheric ozone and aerosol observations: the Alaskan Arctic, *J. Geophys. Res.*, this issue.

Hansen, J., G. Russell, D. Rind, P. Stone, A. Lacis, S. Lebedeff, R. Ruedy, and L. Travis, Efficient three-dimensional global models for climate studies: Models I and II, *Mon. Weather Rev., 111*, 609-662, 1983.

Hicks, B. B., and R. T. McMillen, On the measurement of dry deposition using imperfect sensors and in non-ideal terrain, *Boundary Layer Meteorol., 42*, 79-94, 1988.

Hicks, B. B., D. D. Baldocchi, T. P. Meyers, D. R. Matt, and R. P. Hosker, A multiple preliminary resistance routine for deriving dry deposition velocities from measured quantities, *Water Air Soil Pollut., 36*, 311-330, 1987.

Jacob, D. J., et al., Summertime photochemistry of the troposphere at high northern latitudes, *J. Geophys. Res.*, this issue.

Kawa, S. R., and R. Pearson, Jr., Ozone budgets from the dynamics and chemistry of marine stratocumulus experiment, *J. Geophys. Res., 94*, 9809-9817, 1989.

Kelley, J. J., Jr., and J. D. McTaggart-Cowan, Vertical gradient of net oxidant near the ground surface at Barrow, Alaska, *J. Geophys. Res., 73*, 3328-3330, 1968.

Lechowicz, M. J., The effect of climatic pattern on lichen productivity: *Cetraria cucullata* (Bell.) Ach. in the arctic tundra of northern Alaska, *Oecologia (Berlin), 50*, 210-216, 1981.

Lechowicz, M. J., Ecological trends in lichen photosynthesis, *Oecologia (Berlin), 53*, 330-336, 1982.

Lenschow, D. H., Reactive trace species in the boundary layer from a micrometeorological perspective, *J. Meterol. Soc. Jpn., 60*, 472-480, 1982.

Logan, J. A., Tropospheric ozone: Seasonal behavior, trends and anthropogenic influence, *J. Geophys. Res., 90*, 10,463-10,482, 1985.

Matthews, E., Global vegetation and land use: new high-resolution data bases for climate studies, *J. Clim. Appl. Meteorol.*,, 22, 474-487, 1983.

McMillen, R. T., An eddy correlation technique with extended applicability to non-simple terrain, *Boundary Layer Meteorol., 43*, 231-245, 1988.

Miller, P. C., W. A. Stoner, and L. L. Tieszen, A model of stand photosynthesis for the wet meadow tundra at Barrow, Alaska, *Ecology, 57*, 411-430, 1976.

Oechel, W. C., Seasonal patterns of temperature response of CO_2 flux and acclimation in arctic mosses growing in situ, *Photosynthetica, 10*, 447-456, 1976.

Oltmans, S. J., and W. D. Komhyr, Surface ozone distributions and variations from 1973-1984 measurements at the NOAA Geophysical Monitoring for Climatic Change Baseline Observatories, *J. Geophys. Res., 91*, 5229-5236, 1986.

Ritter, J. A., J. D. W. Barrick, G. W. Sachse, G. L. Gregory, M. A. Woerner, C. E. Watson, G. F. Hill, and J. E. Collins, Airborne flux measurements of trace species in an Arctic boundary layer, *J. Geophys. Res.*, this issue.

Sandholm, S.T., et al., Tropospheric observations related to N_xO_y distributions and partitioning over the Alaskan Arctic, *Journal of Geophysical Research*, this issue.

Singh, H. B., D. O'Hara, D. Herlth, J. D. Bradshaw, S. T. Sandholm, G. L. Gregory, G. W. Sachse, D. R. Blake, P. J. Crutzen, and M. A. Kanakidou, Atmospheric measurements of peroxyacetyl nitrate and other organic nitrates at high latitudes: Possible sources and sinks, *J. Geophys. Res.*, this issue.

Stoner, W. A., and P. C. Miller, Water relations of plant species in the wet coastal tundra at Barrow, Alaska, *Arctic Alpine Res., 7*, 109-124, 1975.

Wesely, M. L., Parameterization of surface resistance to gaseous dry deposition in regional-scale numerical models, *Atmos. Environ., 23*, 1293-1304, 1989.

Wesely, M. L., and B. B. Hicks, Some factors that affect the deposition rates of sulfur dioxide and similar gases on vegetation, *J. Air Pollut. Contr. Assoc., 27*, 1110-1116, 1977.

Wesely, M. L., D. R. Cook, and R. M. Williams, Field measurement of small ozone fluxes to snow, wet bare soil, and lake water, *Boundary Layer Meteorol., 20*, 459-471, 1981.

P. S. Bakwin, S.-M. Fan, D. J. Jacob, P. A. Spiro, and S. C. Wofsy, Department of Earth and Planetary Sciences and Division of Applied Sciences, Harvard University, Cambridge, MA 02138.

E. V. Browell, G. L. Gregory, and J. Ritter, NASA Langley Research Center, Hampton, VA 23665.

D. R. Fitzjarrald and K. E. Moore, Atmospheric Sciences research Center, SUNY Albany, Albany, NY 10025.

(Received February 12, 1991;
revised September 30, 1991;
accepted October 25, 1991.)